Annealing behavior of neon-implanted magnetic garnet

H. Awano,[a] V. S. Speriosu, and C. H. Wilts
California Institute of Technology, Pasadena, California 91125

(Received 12 September 1983; accepted for publication 22 November 1983)

Ferromagnetic resonance spectra and x-ray rocking curves were used to measure the change in magnetic properties and strain with annealing temperature in the surface layer of (111)-oriented Gd, Tm, Ga substituted yttrium iron garnet films implanted with Ne^+ at 190 keV. For doses below about 4×10^{14} ions/cm^2, the entire implanted layer remains crystalline and magnetic. The implantation-induced strain decreases monotonically with increasing annealing temperature, falling to zero at a temperature of 1100 °C. The implantation-induced magnetic anisotropy varies with strain in the same manner as for unannealed material until the annealing temperature reaches 800 °C. For higher temperatures, the anisotropy has a value larger than that expected for unannealed material. At a higher dose, 5×10^{14} ions/cm^2, the center of the implanted region is both amorphous and nonferrimagnetic. Single-crystal order and ferrimagnetism return with annealing near 500 °C. The magnetization and exchange constant decrease with increasing dose, and annealing at 1100 °C restores them to bulk values.

PACS numbers: 75.70.Dp, 76.50. + g, 81.40.Ef, 75.30.Kz

I. INTRODUCTION

It is well known that ion implantation of single-crystal garnets introduces a strain and change in magnetic anisotropy and that subsequent annealing modifies both strain and anisotropy.[1–4] One goal of this investigation was to quantify the effect of annealing for low doses by obtaining depth profiles of strain and anisotropy as a function of annealing temperature. For high doses it is known that the implanted layer may become nonferrimagnetic as well as amorphous. A second goal was to study the regrowth of both crystalline and magnetic properties for such high-dose implants. In an earlier paper we have reported the dependence of strain, damage, and magnetic profiles on dose for garnet films implanted with neon, helium, and hydrogen.[4] In this paper we examine the effects of subsequent annealing on those films which were implanted with neon. Helium implantation was not included because of the formation of bubbles when annealing high-dose samples. Hydrogen implants were also excluded because of special problems associated with the high concentration of relatively mobile hydrogen atoms.

From the point of view of applications, the most important property is the local change in the total magnetic anisotropy, which has three principal components, uniaxial, cubic crystalline, and shape anisotropy. In practical bubble materials, the largest component is the change in uniaxial anisotropy ΔH_k. A convenient measure of the total is obtained from the change in local uniform resonance field which is determined experimentally from analysis of the ferromagnetic resonance (FMR) spectra in the perpendicular configuration

$$\Delta H_{un} = \Delta(\omega/\gamma) - (\Delta H_k - \Delta 4\pi M - \tfrac{2}{3}\Delta H_1).$$

Since there is negligible change in γ or g,[4] the change in perpendicular magnetic anisotropy is directly measured by the change in local uniform resonance field, and it is this latter quantity which is obtained with greatest accuracy (often approaching 1%) from FMR analysis.

From the standpoint of physical understanding, a separation of the individual components is desirable but experimentally difficult. The change in magnetization, $\Delta 4\pi M$, can be obtained by matching mode amplitudes.[4] Here the accuracy in $4\pi M$ is only 10% and at times as poor as 20% so that $\Delta 4\pi M$ cannot be accurately specified. The change in H_1 is even more elusive. For a uniform film, analysis of FMR as a function of field angle permits measurement of H_1 to an accuracy of a few Oe, but for an implanted layer such measurement and analysis only permit an estimate of the value in the surface layer with accuracy of perhaps 50 Oe. For these reasons, only values of ΔH_{un} will be given in this paper. However, it is important to note that ΔH_k is usually by far the largest of the three components.

The garnet used in this study was a narrow-linewidth (111)-oriented Gd, Tm, Ga substituted yttrium iron garnet (Gd, Tm, Ga:YIG) implanted with neon at 190 keV with dose ranging from 5×10^{13} to 5×10^{14} ions/cm^2. Physical and magnetic properties of the four samples used are given in Table I. The experimental tools were x-ray rocking curves to determine strain profiles and ferromagnetic resonance to determine magnetic properties. The as-grown crystal had a perpendicular strain of 0.07% relative to the GGG substrate, and implantation resulted in an increase in this strain. In Ref. 4 and in this paper, the strain in the implanted layer is given relative to the bulk or underlying unimplanted layer of the magnetic garnet, in other words, the increase above the original value of 0.07%. Figures 1 and 2 give an abbreviated picture of the properties of neon implantation before annealing, as reported in Ref. 4. Figure 1 gives the variation of ΔH_{un} and $4\pi M$ with strain in the region of maximum strain in the implanted layer. The change in magnetic anisotropy is initially linear with strain, followed by saturation at a strain of about 1.2%. For higher dose and strain the anisotropy

[a] On leave from Sony Corporation, Tokyo, Japan.

 0021-8979/84/083043-06$02.40

TABLE I. Physical and magnetic properties of garnet films.

Nominal composition $(Gd_{0.84}Tm_{1.17}Y_{0.99})(Fe_2)$ $(Ga_{0.39}Fe_{2.61})O_{12}$	
Nominal thickness (μm)	0.95
$4\pi M$ (G)	515
g	1.71
A(erg/cm)	2.9×10^{-7}
H_1 (Oe)	-165
H_k (Oe)	610
Crystal strain (as-grown)	0.07%
Implant conditions	
Ion	Ne^+
Nominal energy (keV)	190
Nominal doses (ions/cm^2)	5×10^{13}
	1×10^{14}
	3×10^{14}
	5×10^{14}

decreases to zero as the material becomes paramagnetic at a strain of 1.8%. The crystal becomes locally amorphous when the strain exceeds about 2.5%. The magnetostrictive component of anisotropy can be calculated from the equation

$$\frac{\Delta H_k}{\Delta\epsilon^{\perp}} = \frac{3E\lambda_{111}}{M(1+\nu)}.$$

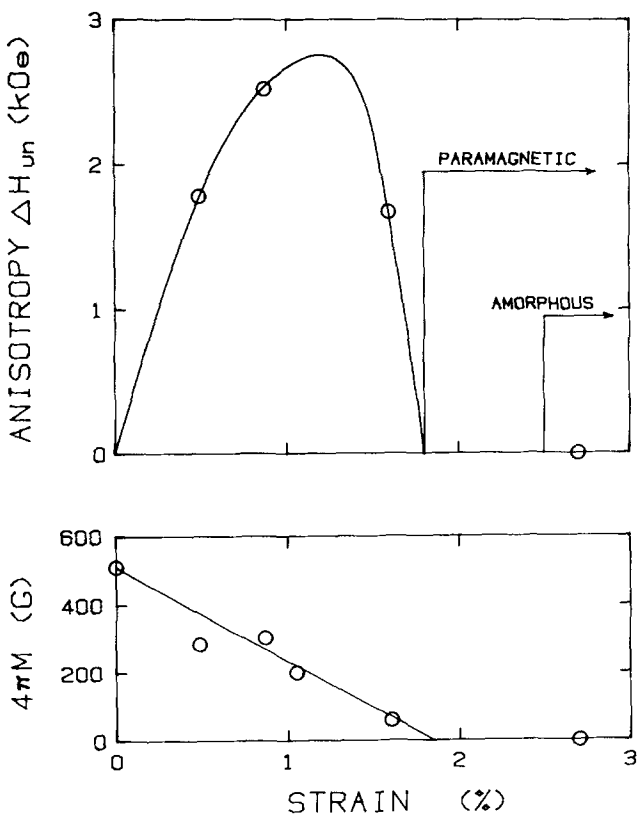

FIG. 1. Magnetization and change in magnetic anisotropy as a function of strain in the region of maximum strain. Implantation is neon at an energy of 190 keV (from Ref. 4).

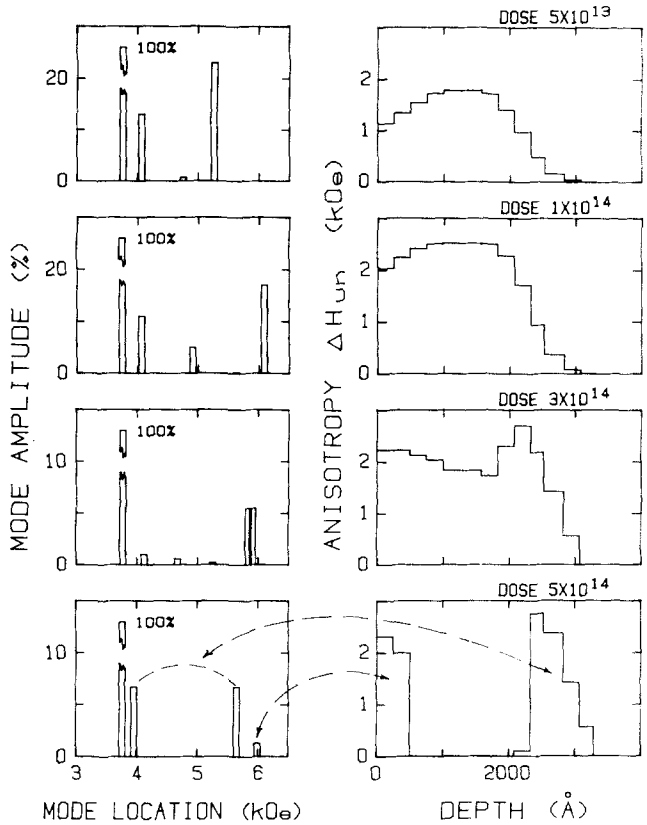

FIG. 2. Perpendicular FMR spectra and magnetic anisotropy profiles for neon implantation at 190 keV. Implantation dose varies from 5×10^{13} to 5×10^{14} ions/cm^2. The large (100%) mode is the main resonance of the unimplanted layer. The other modes are surface modes (from Ref. 4).

If the initial linear slope of 4.1 kOe per percent is attributed to this effect, with $E = 2(10)^{12}$ dyn/cm^2 and $\nu = 0.29$, the magnetostrictive constant is predicted to be $\lambda_{111} = -3.6\times10^{-6}$. Since λ_{111} is not known for this composition, it can only be crudely estimated by White's method[5] using tabulated values for unsubstituted garnets.[6] This gives the value $\lambda_{111} = -3.1\times10^{-6}$, which was erroneously reported as -3.4×10^{-6} in Ref. 4. The accuracy of this method can be checked using (Ga:YIG) where experimental data are available, and λ is of the same order of magnitude. Deviations between calculated and experimental values range from 0.4×10^{-6} to 0.5×10^{-6} for λ_{111} and to more than 1.0×10^{-6} for λ_{100}. Clearly the 15% difference observed above lies within this range, leading to the conclusion that for low doses the entire change in anisotropy may be attributable to magnetostriction but that a 10% or 20% contribution due to other sources cannot be ruled out. Using the above value of λ_{111}, and values of H_k and bulk crystal strain from Table I, it is readily shown that the original growth-induced anisotropy is about 900 Oe. Figure 2 gives FMR spectra and the corresponding magnetic anisotropy profiles which have a single peak for low dose, a bimodal shape for medium dose, and two magnetic layers separated by nonmagnetic (paramagnetic) layer at high dose. At still higher doses, the outer surface also becomes nonmagnetic, leaving a narrow layer of damaged but magnetic material near the interface with unimplanted material.

II. EXPERIMENT

In the present study, each film was annealed for 30 min in air at successively higher temperatures from 300° to 1100°, usually at 100° intervals. Bragg case double-crystal Cu $K\alpha$(444) or (888) x-ray rocking curves and FMR spectra using a 10-GHz cavity spectrometer were obtained after each anneal. In some regions where the spectrum was changing rapidly the interval was reduced to 50 °C. At an annealing temperature of 1100°, the x-ray rocking curve showed that the strain induced by implantation had decreased to zero (resolution better than 0.01%) and the tests were terminated. Strain and magnetic profiles were obtained using the method described in Ref. 4.

III. RESULTS

Typical results are shown in Fig. 3(a)–3(d), where strain and anisotropy profiles are plotted toghether. In these figures, the strain has been multiplied by 4.1 kOe per percent, the initial slope of Fig. 1. As explained earlier this slope is consistent with a magnetostrictive origin for ΔH_{un} and use of this factor ensures that the plotted profiles will be identical for unannealed samples at low values of strain. Deviations between the two profiles will then show regions where strain and anisotropy are no longer linearly related.

The region of maximum strain is seen to be about 1300 Å below the surface. For low-dose implantation, both strain and anisotropy in this region decrease steadily with increasing annealing temperature as shown in Fig. 4. For higher doses where the anisotropy has passed the peak value, the strain still shows a steady decrease,but the anisotropy first returns to a value near the peak of Fig. 1 and then decreases. It is also seen in Fig. 4 that the bulk resonance remains unchanged up to 900 °C, with a monotonic decrease of 270 Oe between 900 and 1100 °C. Constancy of bulk mode amplitude indicates no change in $4\pi M$, and measurements for a few selected cases showed also that the bulk values of H_1 and γ had not changed significantly. The change in bulk resonance must be primarily due to an increase in the uniaxial anisotropy. The unusual small dip seen between 800 and 900 °C appeared consistently in three samples. Unfortunately data are not available at these temperatures for the two lowest doses so it is not known if the same feature shown there by a dotted line is correct.

A cursory examination of Figs. 3 and 4 shows that in the region of peak strain, the relation between anisotropy and strain during annealing roughly follows the curve of Fig. 1, but there are some significant differences. This is best shown by superimposing plotted points of anisotropy vs strain on Fig. 1. Results are shown in Fig. 5. Each graph gives data for a different implantation dose, with a sequence of points corresponding to different annealing temperatures, starting at room temperature and ending at 1100 °C where the strain has decreased to zero. For all but the highest dose, the points

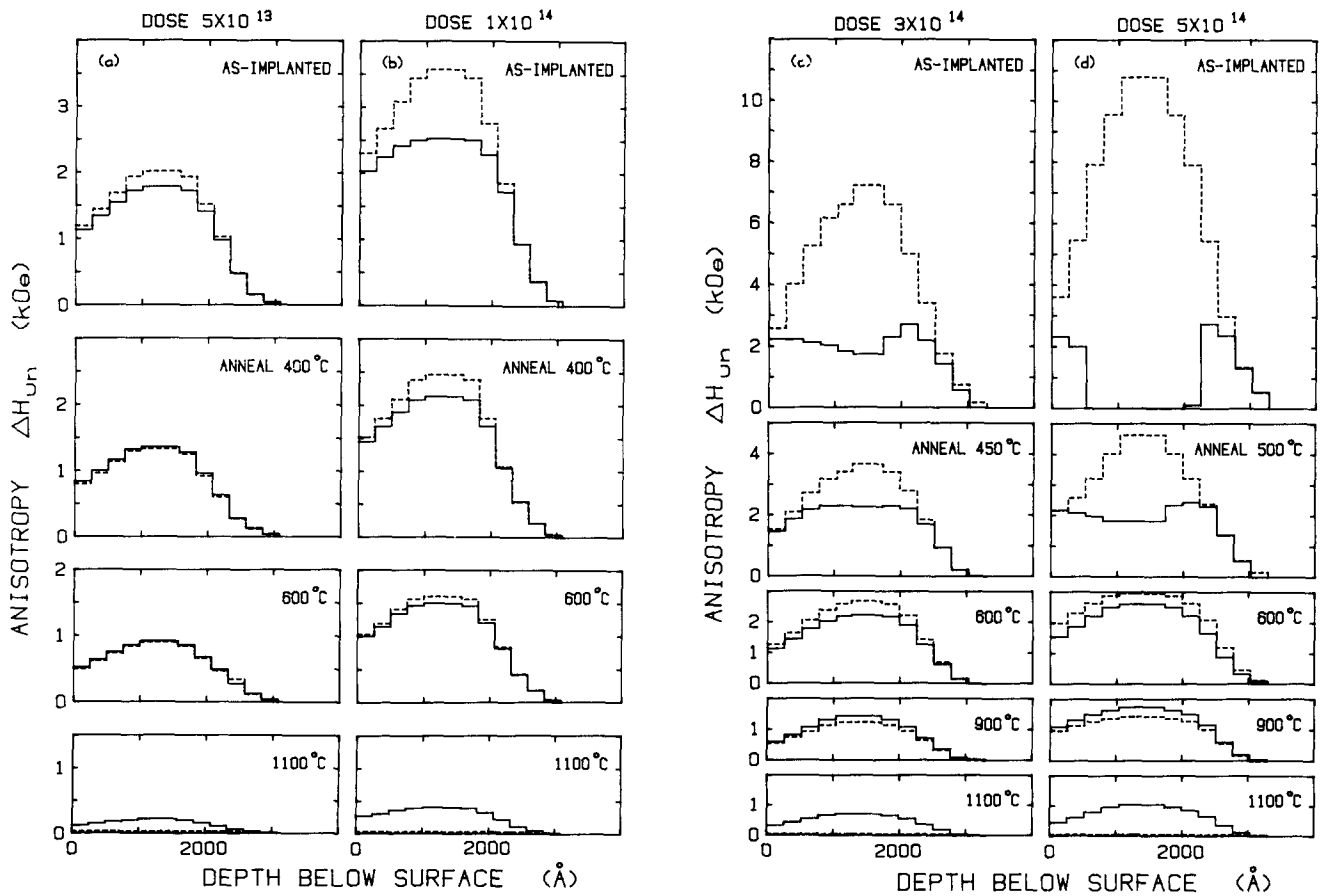

FIG. 3. Profiles of magnetic anisotropy ΔH_{un} (solid line) and strain (dotted line) for a number of annealing temperatures between room temperature and 1100 °C. Strain has been multiplied by 4100 for ease of comparison with ΔH_{un}.

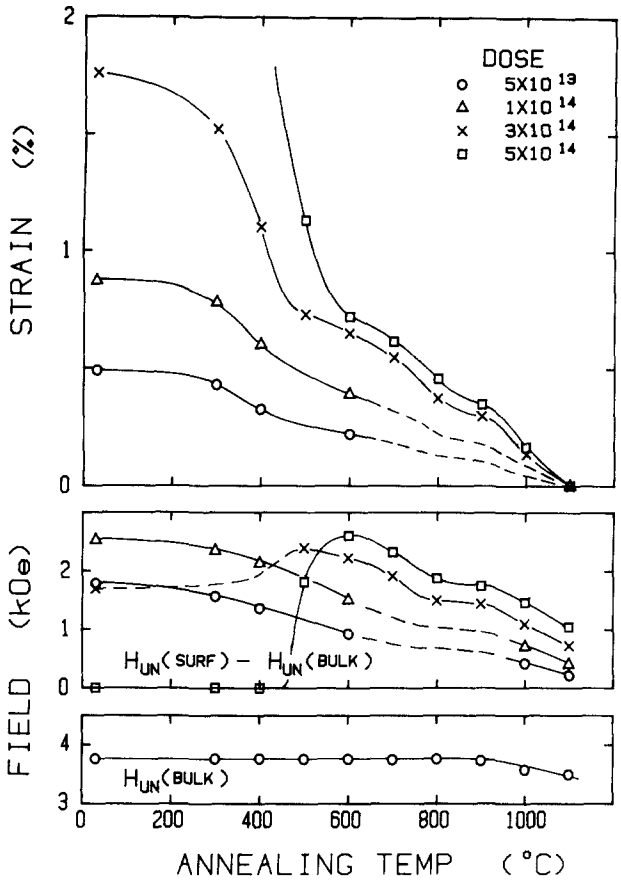

FIG. 4. Strain and change in magnetic anisotropy at the depth of maximum strain as functions of annealing temperature. Uniform resonance field for unimplanted (bulk) region is also shown.

follow the curve of Fig. 1 closely except for a deviation above 800 °C which will be discussed later.

For the sample with highest dose the region of maximum damage was both nonmagnetic and amorphous before annealing. Between 400° and 500° this region became crystalline and magnetic (though not necessarily at the same temperature) and at 600° the material had a peak anisotropy about 250 Oe larger than the corresponding point of Fig. 1. The anisotropy remained above the line of Fig. 1 until a temperature of 800° was exceeded, beyond which a greater deviation was observed similar to that seen in the other samples. Above 800°, all experimental data deviate from Fig. 1 by an amount that increases both with dose and temperature. The maximum deviation at 1100° (where the strain is now zero) appears to vary roughly linearly with the maximum strain (before annealing) and has a peak value of about 1000 Oe at the highest dose.

The regrowth of magnetic properties is the most interesting feature of the highest-dose case. Figure 6 shows the location of the FMR surface modes as a function of annealing temperature. The main resonance of the unimplanted material is at the bottom of the figure. Surface mode amplitude as a percent of this main resonance is printed beside each plotted point. Before annealing there are only three surface modes with very small amplitude. This mode structure requires an implanted layer consisting of a nonmagnetic region separating two magnetic layers. As the annealing temperature is increased to 450 °C, the modes shift very little, but their amplitudes increase. This shows that the peak anisotropy is not changing much, but the saturation magnetization or the thickness of the magnetic layers is increasing or both.

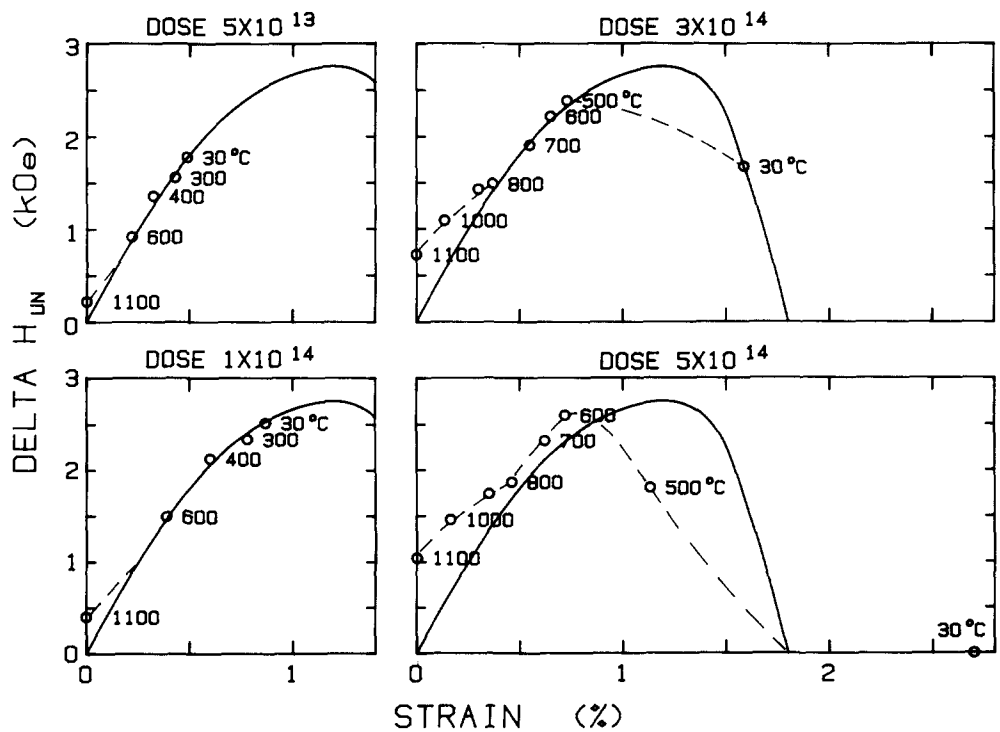

FIG. 5. Change in magnetic anisotropy ΔH_{un} vs strain at depth of maximum strain.

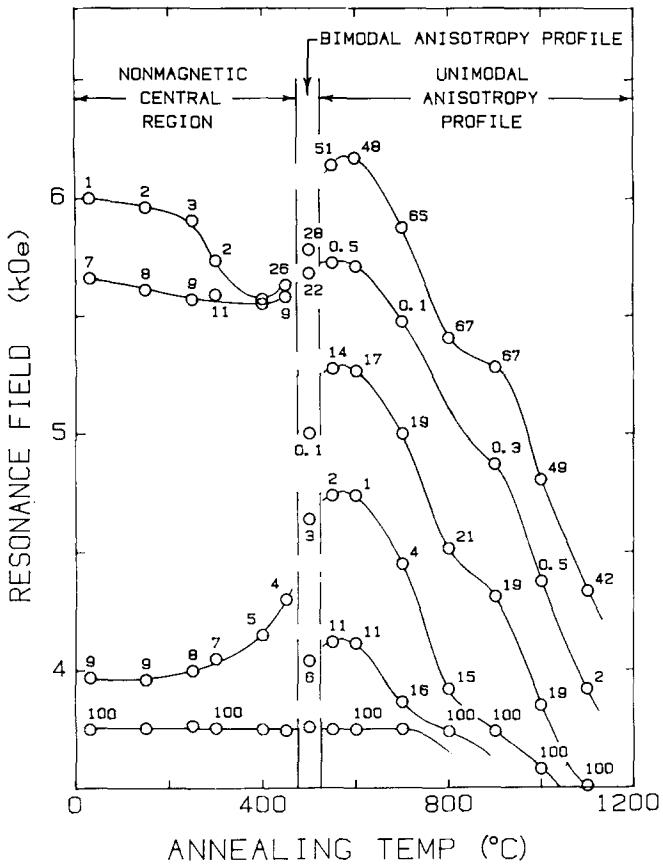

FIG. 6. Perpendicular FMR spectrum for highest-dose case as a function of annealing temperature. Mode amplitude in percent is given by number beside each point. The 100% mode is the main resonance of the unimplanted layer; the other modes are surface modes.

At 500° there is a drastic change in mode structure and five surface modes are evident. This requires that the nonmagnetic region has become magnetic but the anisotropy profile is still bimodal. Above 550° the spectrum becomes characteristic of an unimodal anisotropy profile. The transition is very rapid from a definitely nonmagnetic region at 450 °C to a continuous but bimodal profile at 500 °C to an unimodal profile at 550 °C.

The last figure (Fig. 7) shows the change in saturation magnetization and exchange constant A with annealing temperature in the region where the strain has the maximum value. Because of difficulty in accurate measurement of mode amplitudes, the values of $4\pi M$ are not as accurate as the anisotropy and strain values. We estimate the accuracy to be $+20\%$. For low doses the magnetization is initially lower than bulk value, but becomes equal to the bulk value when the annealing temperature reaches about 600°. For the highest dose, the nonmagnetic layer becomes magnetic at 500 °C and at 600 °C the magnetization appears to reach a value 20 or 30% larger than the bulk value. It decreases to the bulk value when the annealing temperature reaches 1000 °C.

The value of exchange, A, has comparable accuracy at low annealing temperatures where a large number of modes is observed. However, for the low-dose cases, only two surface modes remain at 1000 °C anneal, and it is only in the high-dose case that A can be measured with any accuracy.

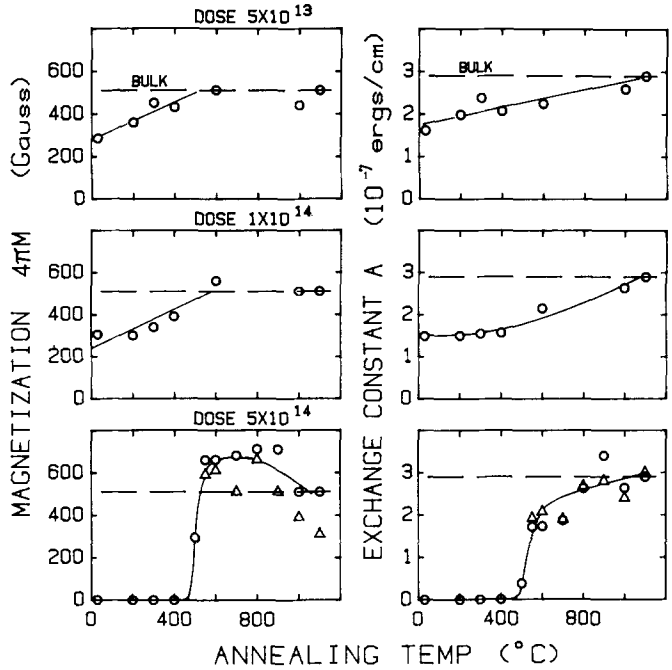

FIG. 7. Variation of magnetization, $4\pi M$, and exchange constant, A, with annealing temperature.

Nevertheless it is clear that A does not return to the bulk value at 500°, and it appears to reach this value at annealing temperature of about 1000 °C.

IV. DISCUSSION

For strain values below 1.2%, for which the anisotropy increases with strain everywhere, and for annealing temperatures below 800 °C, the behavior of ΔH_{un} with strain does not depend on whether the change in strain is obtained by a change in ion dose or by a change in annealing temperature. For strain values greater than 1.2% but below 1.8% (where the material becomes paramagnetic but not amorphous), the relationship between ΔH_{un} and strain with annealing temperature is initially different from that obtained by implantation alone. However, between 500° and 800 °C ΔH_{un} vs strain again follows the curve for unannealed material. Thus if the initial damage was insufficient to create amorphousness, there is a range of annealing temperature for which the damage created by an increase in ion dose appears to be reversible by annealing at a higher temperature.

For the highest-dose case, where the region of highest damage reached amorphousness, annealing between 600° and 800° results in a 250-Oe shift in the relation between ΔH_{un} and strain. This indicates that some of the magnetic properties are different after regrowth of the crystal structure. The shift observed is in the direction of an increase in $4\pi M$ or a destruction of growth-induced anisotropy. In Fig. 7 we have shown an increase in $4\pi M$ of about 150 Oe in this temperature range. Since the accuracy in measuring the local value of $4\pi M$ lies in the range of 10 or 20%, we are not certain that this increase is real, but it is roughly comparable to the 250-Oe shift in Fig. 5. This implies that after regrowth the anisotropy not related to strain or saturation differs by

only 100 Oe from the original growth-induced anisotropy. Since the probable error is larger than 100 Oe, there is no confidence in this numerical value, but it is clearly small compared to the original value of this anisotropy which was shown earlier to be about 900 Oe.

It may seem surprising that regrowth of the crystal structure would restore the anisotropy to its original value. Our definition of amorphousness is tied to the intensity observed in experimental Cu $K\alpha$ (444) rocking curves.[4] For this reflection the dominant contribution to the structure factor comes from the c sublattice occupied by rare-earth and yttrium ions. The rare-earth ions are also the dominant contributors to magnetostriction and anisotropy.[6] The preimplantation growth-induced uniaxial anisotropy is attributed to preferential uniaxial ordering of the rare-earth atoms during liquid-phase epitaxial growth. With implantation and increasing strain the structure factor diminishes, corresponding to random displacements of the c-sublattice atoms. For Ne^+ implantation as the peak strain reaches 2.5%, the intensity diffracted from the region of peak strain reaches the noise level. Hence we identify this damage level as corresponding to amorphousness. It is probable that this damage level is different from that identified with amorphousness by other techniques such as electron diffraction. It is also probable that either technique underestimates the damage level for which there is no long-range order (i.e., true amorphousness). Another plausible reason for the regrowth of strain-unrelated anisotropy is that upon annealing, the uniaxial ordering of rare-earth ions is propagated during the solid-phase epitaxy. Due to uncertainty in the original magnetostriction constant and lack of knowledge of its local variation, it is not possible to further elucidate the details of magnetic variations with implantation and annealing. In particular we do not know how to interpret the excess ΔH_{un} observed in every case after annealing at more than 800 °C. In this temperature range the situation is further complicated by the changes undergone by the unimplanted bulk.

ACKNOWLEDGMENTS

We thank the San Jose laboratory of IBM for providing the implanted garnet samples and encouraging this study, and also Rockwell International for providing access to a double-crystal diffractometer. A preliminary presentation of some of the experimental data in this paper was made at the 1983 International Magnetics Conference in Philadelphia, Pennsylvania.

[1] J. C. North and R. Wolfe, in *Ion-Implantation in Semiconductors and Other Materials*, edited by B. L. Crowder (Plenum, New York, 1973).
[2] K. Komenou, I. Hirai, K. Asama, and M. Sakai, J. Appl. Phys. **49**, 5816 (1978).
[3] G. P. Vella-Coleiro, R. Wolfe, S. L. Blank, R. Caruso, T. J. Nelson, and V. V. S. Rana, J. Appl. Phys. **52**, 2355 (1981).
[4] V. S. Speriosu and C. H. Wilts, J. Appl. Phys. **54**, 3325 (1983).
[5] R. L. White, IEEE Trans. Magn. **MAG-9**, 606 (1973).
[6] P. Hansen, in *Physics of Magnetic Garnets*, edited by A. Paoletti (North-Holland, New York, 1978), pp. 75–76.